IAI Journals.ASM.org

The Makes Caterpillars Floppy (MCF)-Like Domain of *Vibrio vulnificus* Induces Mitochondrion-Mediated Apoptosis

Shivangi Agarwal,[a] Yeuming Zhu,[b] David R. Gius,[b] Karla J. F. Satchell[a]

Department of Microbiology-Immunology[a] and Department of Radiation Oncology,[b] Feinberg School of Medicine, Northwestern University, Chicago, Illinois, USA

The multifunctional-autoprocessing repeats-in-toxin ($MARTX_{Vv}$) toxin of *Vibrio vulnificus* plays a significant role in the pathogenesis of this bacterium through delivery of up to five effector domains to the host cells. Previous studies have established that the $MARTX_{Vv}$ toxin is linked to *V. vulnificus* dependent induction of apoptosis, but the region of the large multifunction protein essential for this activity was not previously identified. Recently, we showed that the Makes Caterpillar Floppy-like MARTX effector domain (MCF_{Vv}) is an autoproteolytic cysteine protease that induces rounding of various cell types. In this study, we demonstrate that cell rounding induced by MCF_{Vv} is coupled to reduced metabolic rate and inhibition of cellular proliferation. Moreover, delivery of MCF_{Vv} into host cells either as a fusion to the N-terminal fragment of anthrax toxin lethal factor or when naturally delivered as a *V. vulnificus* MARTX toxin led to loss of mitochondrial membrane potential, release of cytochrome *c*, activation of Bax and Bak, and processing of caspases and poly-(ADP-ribose) polymerase (PARP-γ). These studies specifically link the MCF_{Vv} effector domain to induction of the intrinsic apoptosis pathway by *V. vulnificus*.

Vibrio vulnificus, a motile Gram-negative halophilic foodborne pathogen, is the causative agent of fatal fulminant septicemia and gastroenteritis following ingestion of contaminated seafood. In addition, skin and soft tissue wound infections like necrotizing fasciitis can occur in high-risk immunocompromised subjects, with mortality rates as high as 50% (1, 2). The severity of the disease acquired by either the oral or wound route of infection is due to secreted toxins that both reduce innate immune cells at the site of infection to promote bacterial growth and induce tissue necrosis, providing a route for systemic spread (3–9).

The ability of the bacterium to induce tissue necrosis is specifically attributed to two cytotoxins: the cytolytic pore-forming *V. vulnificus* cytolysin (VVC), encoded by the gene *vvhA*, and the multifunctional autoprocessing repeats-in-toxin ($MARTX_{Vv}$) toxin, encoded by the gene *rtxA1* (4, 7, 9). In addition to necrosis, *V. vulnificus* has been reported to induce apoptosis both *in vitro* and *in vivo*, resulting in depletion of lymphocytes (10, 11). Studies using purified protein have established that rVVC induces the intrinsic pathway of apoptosis, as indicated by increased detection of Bax and processing of caspases 9 and 3 but not caspase 8 (12–14). Purified extracellular protease rVvpM has also been shown to induce apoptosis with release of cytochrome *c* and activation of caspases 9 and 3 (15).

In contrast, studies using coincubation of live *V. vulnificus* have demonstrated that the bacteria induce apoptosis and that this activity is dependent primarily upon an intact *rtxA1* gene as well upon the toxin secretion gene *rtxE* (5, 16). Only when the bacteria produce the $MARTX_{Vv}$ toxin are there a significant reduction in mitochondrial membrane potential, release of cytochrome *c*, and processing of caspase 3, despite the presence of intact *vvhA* and *vvpM* genes in these bacteria. This ability of *V. vulnificus* to induce mitochondrial damage during coculture was shown further to depend upon the presence of Ca^{2+} in the medium (17), which was recently shown to be essential for secretion of the $MARTX_{Vv}$ toxin from *V. vulnificus* (18), recapitulating the linkage of the $MARTX_{Vv}$ toxin to mitochondrial damage.

$MARTX_{Vv}$ is a large composite holotoxin comprised of long repeat regions at the N and C termini. The repeat regions form a pore at the eukaryotic plasma membrane that is proposed to translocate up to five distinct effector domains across the eukaryotic plasma membrane (18, 19). These effector domains are then released into the cytosol by induction of the autoprocessing cysteine protease domain (CPD) that is stimulated by the small molecule inositol hexakisphosphate (18, 20). It has been shown that the repeat regions are sufficient for pore formation and necrosis but that the effector domains are required for the cytopathic activities of the cell, including cell rounding (18).

Among the eight potential effector domains carried by $MARTX_{Vv}$ toxins of various isolates (21–23), a ubiquitous effector domain carried by all clinical biotype 1 *V. vulnificus* strains and by biotype 2 strains that infect eels is the Makes Caterpillars Floppy-like (MCF_{Vv}) domain (Fig. 1) (19, 21, 22). This 376-amino-acid domain shares homology with internal domains of other large bacterial toxins, including *Photorhabdus* Makes Caterpillar Floppy toxins Mcf1 and Mcf2 and *Pseudomonas fluorescens* FitD toxin (24, 25). MCF_{Vv} has recently been shown to be an autoproteolytic cysteine protease that is activated by an as-yet-unidentified heat-resistant proteinaceous component from host cell lysate (26). This suggests that one function of this domain in other large toxins like Mcf1 and FitD is as an autoproteolytic domain to autoprocess the large toxins during toxin translocation. In addition to autoproteolysis, MCF_{Vv} was further shown to induce a cytopathic effect in cells typified by rounding of different cell type, and this cytopathicity depended upon a catalytic site composed of ar-

Received 3 May 2015 **Returned for modification** 5 June 2015
Accepted 26 August 2015
Accepted manuscript posted online 8 September 2015
Citation Agarwal S, Zhu Y, Gius DR, Satchell KJF. 2015. The Makes Caterpillars Floppy (MCF)-like domain of *Vibrio vulnificus* induces mitochondrion-mediated apoptosis. Infect Immun 83:4392–4403. doi:10.1128/IAI.00570-15.
Editor: S. M. Payne
Address correspondence to Karla J. F. Satchell, k-satchell@northwestern.edu.

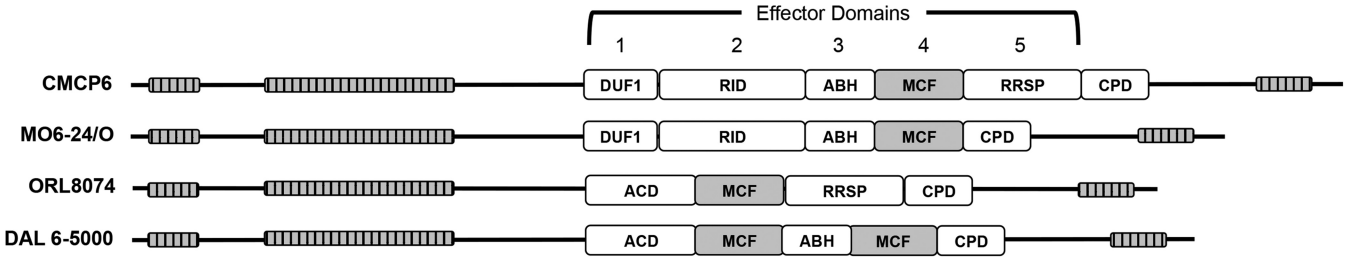

FIG 1 Schematic diagrams of $MARTX_{Vv}$ toxins from representative clinical biotype 1 *V. vulnificus* strains (indicated on the left) showing distinct arrangements of effector domains. Effector domains are designated domain of unknown function in the first position (DUF1), Rho inactivation domain (RID), alpha-beta hydrolase (ABH), Makes Caterpillars Floppy-like (MCF), Ras/Rap1-specific protease (RRSP), and the cysteine protease domain (CPD). Note that MCF (gray) is the only domain present in all variants. The arrangements here are based on sequencing found in the work of Kwak et al. (21).

ginine-3350, cysteine-3351, and aspartate-3352 residues arranged in tandem (26).

Although this domain derived its name from the *Photorhabdus* Makes Caterpillar Floppy toxins Mcf1 and Mcf2, a similar cytopathic effect was not observed when the aligned region of the large Mcf1 toxin was transfected into cells (26). Indeed, while Mcf1 has been linked to induction of apoptosis, the BH3 domain essential for induction of apoptosis by the large Mcf1 toxin maps outside the region that aligns with MCF_{Vv} (24, 27). An alternative model has suggested that Mcf1 is essential to inactive Rac1 in the host cells (28), although the portion of the 2,929-amino-acid toxin required for this inactivation is not yet mapped. Thus, there is little information in the literature to suggest the mechanism by which MCF_{Vv} induces cytopathicity. Therefore, this study was conducted to investigate the process of MCF_{Vv}-mediated cytopathicity. We demonstrate that MCF_{Vv} is the effector domain of the $MARTX_{Vv}$ toxin that induces depolarization of mitochondria and activation of the proapoptotic cascade within the host cell. Upon sustained exposure of cells to MCF_{Vv}, the cells become nonviable and fail to proliferate, indicating that MCF_{Vv} is a cytotoxin that induces apoptosis.

MATERIALS AND METHODS

Chemicals, reagents, cell lines, and bacterial strains. Bacterial strains and plasmids used in this study are listed in Table 1. Bacterial strains were grown in Luria-Bertani (LB) broth or agar supplemented with 50 μg/ml rifampin, 5 μg/ml chloramphenicol, 100 μg/ml ampicillin, or 50 μg/ml kanamycin as appropriate. Enzymes for cloning were purchased from New England BioLabs (Beverly, MA), and custom oligonucleotides were from Integrated DNA Technologies (Coralville, IA). DNA sequencing was conducted at the Northwestern University Genomics core facility.

Human cervical epithelial HeLa cells (obtained from ATCC) were cultured at 37°C with 5% CO_2 in Dulbecco's modified Eagle's medium (DMEM, Life Technologies) containing 10% fetal calf serum (Gemini Bio-Products, West Sacramento, CA), 100 U/ml penicillin, and 1 μg/ml streptomycin. Cells were transfected with DNA using FuGENE HD transfection reagent (Promega) at a 1:3 ratio for 18 h. For some transfection experiments, cells were seeded onto coverslips, treated as detailed below, and fixed with paraformaldehyde. Cells were stained with 4′,6-diamidino-2-phenylindole (DAPI) to visualize nuclei and then imaged using a Zeiss LSM510 Meta-UV confocal microscope.

Protein purification and cellular intoxication. Six-His-tagged LF_N, LF_N-MCF_{Vv}, and LF_N-MCF_{C3351A} were purified after overexpression in BL21(λDE3) by nickel affinity chromatography as previously described (26). Anthrax toxin protective antigen (PA) was purified as previously described (26). Cellular intoxications were conducted by adding 168 nM PA to DMEM over cells followed by addition 72 nM LF_N or LF_N fusion protein, and cells were incubated at 37°C with 5% CO_2 for 24 h unless otherwise stated.

MTT assay. The 3-(4,5-dimethylthiazol-2-yl)-2,5-diphenyltetrazolium bromide (MTT) assay used was modified from the protocol by Mosmann (29). HeLa cells were transfected in 96-well dishes as described

TABLE 1 *V. vulnificus* strains, plasmids, and oligonucleotide primers used in the study

Strain, plasmid, or oligonucleotide	Relevant characteristic or sequence[a]	Reference
Strains		
BS1405	CMCP6 Δ*vvhA* Rif^r	18
BS1406	BS1405 Δ*rtxA1* Rif^r	18
BS1407	BS1405 *rtxA1*::*bla* Rif^r	18
SNG1	BS1405 *rtxA1*::*mcf-bla* Rif^r	This study
SNG2	BS1405 *rtxA1*::*mcf*(*C3351A*)-*bla* Rif^r	This study
Plasmids		
pHGJ5	*rtxA1*::*bla*; *sacB*, *ori*R6K Cm^r	18
pSA8	*mcf* in fusion with *bla* in pHGJ5; Cm^r	This study
pSA9	*mcf*(*C3351A*) in fusion with *bla* in pHGJ5; Cm^r	This study
Oligonucleotides (5′-3′)		
1	GAACAG**GTCGAC**GTTCAATGCAGAGCAAGCAGCG	This study
2	GAACAG**GTCGAC**GCCAATGCTTCGAGATCGCTCGC	This study
3	GGTTTTGGTGGGCGTGCTGATCCACTTTCTAAAC	26

[a] Bacterial strains and plasmids used are either Rif^r (rifampin resistant) or Cm^r (chloramphenicol resistant). The enzyme sites in oligonucleotides are in bold. The underlined codon for Cys is exchanged for Ala.

above. Staurosporine (STS; 1 μM) was added to the untransfected cells for 4 h as a positive control for induction of apoptosis. After 18 h transfection, the medium was removed, and cells were washed once with phosphate-buffered saline (PBS; pH 7.4), after which 20 μl of 5 mg/ml of MTT (Sigma) was added to each well and incubated at 37°C with 5% CO_2 for 4 h. The insoluble purple formazan crystals were extracted using acidified isopropanol (0.1 N HCl and 0.1% sodium dodecyl sulfate [SDS]), and the absorbance was read using a Molecular Devices SpectraMax M5 microplate reader at 570 nm. Data were normalized as percent metabolic activity by dividing sample absorbance by the absorbance obtained from untransfected cells. Data are reported as means and standard deviations (SD) for biological triplicate samples.

Clonogenic colony formation assay. HeLa cells were intoxicated with LF_N fusion proteins and PA as described above. After 24 h, intoxicated cells were trypsinized and counted, and 200 or 400 cells were plated in 6-well dishes in complete DMEM. After 14 days, cells were stained using crystal violet, and colonies containing more than 50 cells were counted. Percent clonogenic survival was calculated as number of colonies recovered divided by the initial number of cells seeded × 100. Data are reported as means and SD from four biological replicates, each plated twice.

***In vitro* scratch wound assay.** HeLa cells were grown to 50% confluence in 6-well culture dishes and intoxicated with LF_N fusion proteins and PA as described above. After 24 h, a scratch in the seeded cells was introduced with a pipette tip from top to bottom as described previously (30). The rate of cell migration into the wound was measured as the decrease in the distance between edges, determined by comparing images from the time at which the wound was created and after 24 h. Data are reported as mean percent closure of the scratch and SD for biological triplicate samples.

Construction of MCF_{Vv} in fusion with β-lactamase (Bla). The 1,131 nucleotides (nt) of *rtxA1* corresponding to MCF_{Vv} (nt 9607 to 10737) was amplified from *V. vulnificus* CMCP6 genomic DNA using primers 1 and 2. The amplified fragment was digested with SalI, ligated into plasmid pHGJ5 (18), and transformed into *Escherichia coli* SM10λpir cells to generate pSA8. The plasmid was modified further by site-directed mutagenesis using primers 3 and 4 to introduce the codon for C3351A substitution, and the resulting plasmid, pSA9, was transformed to S17λpir. The plasmids were then transferred by conjugation from S17-1λpir to *V. vulnificus* strain BS1407, a derivative of CMCP6 which has an unmarked deletion to remove the *vvhA* hemolysin gene and in which all *rtxA1* gene sequences for the effector domains are replaced with a promoterless beta-lactamase gene (*bla*) sequence (18). Conjugation was followed by selection for double homologous recombinants using sucrose counterselection as previously described (31). The appropriate strains were confirmed by absence of growth on chloramphenicol and the gain of *mcf* DNA sequences in the correct orientation by PCR and sequencing. The growth rate of the mutants in LB supplemented with rifampin was compared to the isogenic CMCP6Δ*vvhA* parent strain BS1405 and is isogenic derivative BS1406 with a deletion of the entire *rtxA1* gene by monitoring absorbance at 600 nm into stationary phase.

Bla secretion and translocation. Ampicillin resistance of *V. vulnificus* strains was determined using a disk diffusion assay as previously described (18) using AM10 antibiotic disks (Thermo Scientific). Bla translocation into HeLa cells was determined using CCF2-AM as a reporter for flow cytometry conducted as previously described (18). Lysis of cells exposed to *V. vulnificus* at a multiplicity of infection (MOI) of 10 was quantified by lactate dehydrogenase (LDH) release as previously described (18) using a CytoTox 96 nonradioactive cytotoxicity assay kit (Promega, Madison, WI) according to the manufacturer's protocol.

Subcellular fractionation. HeLa cells seeded into 6-well dishes at 5×10^6 cells/well were either intoxicated with LF_N fusion proteins and PA or cocultured with bacterial strains as detailed above. After the time points indicated in the figures, cells were resuspended in plasma membrane permeabilization buffer (200 μg/ml digitonin, 80 mM KCl, 2 mM EDTA) and incubated at 4°C for 5 min. The lysates were centrifuged at 1,500 × *g* for 5 min, and the supernatant was collected as the cytosolic fraction. The pellet was resuspended in cell lysis buffer (50 mM Tris HCl, 150 mM NaCl, 2 mM EDTA, 0.2% Triton X-100, 0.3% NP-40 [pH 7.5]) and incubated at 4°C for 10 min with gentle rocking. The lysates were centrifuged at 16,000 × *g* at 4°C for 10 min and the supernatant was collected as the mitochondrial fraction (32). The purity of the cytosolic and mitochondrial fractions was assessed by immunoblotting with rabbit polyclonal antibodies against actin (1:5,000; Sigma) and CoxIV (4844, 1:1,000; Cell Signaling Technology), respectively.

Western blotting. For Western blots, the primary antibodies used were obtained as follows: monoclonal anti-GFP antibody coupled to horseradish peroxidase (HRP) (1:1,000) from Miltenyi Biotec Inc. (Auburn, CA); antibody sampler kits for apoptosis (9915; 1:1,000) and caspase 8 (9746; 1C12; 1:1,000) from Cell Signaling Technology (Danvers, MA); monoclonal antibodies against BAD C7 (Sc-8044; 1:200), BAK G23 (Sc-832; 1:200), and BAX-HRP N-20 (Sc-493; 1:200) from Santa Cruz Biotechnology (Dallas, TX); and monoclonal antibody against cytochrome *c* (7H8.2C12; 1:100) from BD Pharmingen. HRP-conjugated goat anti-rabbit or anti-mouse secondary antibodies (1:5,000) were obtained from Jackson ImmunoResearch Laboratories (West Grove, PA). SuperSignal West Pico chemiluminescent substrate and autoradiography were used for signal detection on X-ray film. Quantification of detected proteins from two independent experiments was performed from digitally scanned X-ray films followed by analysis using the NIH ImageJ v1.49 software. All data were normalized to detection of actin from a parallel Western blot conducted using the same prepared samples and normalized to a relevant negative control on the same gel, as indicated in the figure legends.

Inhibitor studies. In some cases, caspases were irreversibly inactivated prior to intoxication by treating the cells with a 100 μM concentration of the cell permeative pancaspase inhibitor *N*-benzyloxycarbony-Val-Ala-Asp(*O*-methyl)-fluoromethylketone (z-VAD-fmk; R&D Systems) for 4 h prior to intoxication or STS treatment as described above. Dimethyl sulfoxide (DMSO) used to reconstitute the inhibitor was used as the vehicle control. To activate the extrinsic pathway, cells were treated with 20 μg/ml cycloheximide (Sigma) for 12 h followed by addition of 10 ng/ml tumor necrosis factor alpha (TNF-α; Sigma) for 4 h.

Measuring mitochondrial membrane potential by JC-1 staining. For some assays, 5×10^5 HeLa cells were intoxicated with LF_N fusion proteins in the presence of PA as described above. Alternatively, cells were treated with *V. vulnificus* strains at an MOI of 10 for 60 min as described for the translocation assay, but followed by the addition of 100 μg/ml gentamicin for 30 min. Supernatants were collected to quantify LDH release as described above. The treated cells were stained with a 2 μM concentration of the cationic carbocyanine dye JC-1 (Molecular Probes) according to the manufacturer's protocol. The cells were imaged for green versus orange J aggregates using a Zeiss LSM510 Meta-UV confocal microscope. The same samples were quantified for fluorescence using a Molecular Devices SpectraMax M5 microplate reader at excitation/emission wavelengths of 485/535 nm (green; depolarized monomer) and 535/595 nm (red; hyperpolarized J aggregates). Data are reported as the ratio of red to green, with an excess of green (low ratio) indicating apoptotic cells and an excess of red (high ratio) indicating healthy cells.

Computational and statistical analyses. Images from confocal microscopy were processed using Zeiss LSM Image Browser V4.2 software. All data were graphed and analyzed using GraphPad Prism 6 software for Macintosh (San Diego, CA). Statistical significance for experiments was determined by analysis of variance (ANOVA) followed by multiple-comparison tests for all experiments conducted in at least triplicate.

RESULTS

Ectopic expression of MCF_{Vv} results in loss of host metabolic activity. Previously, we established that cells transfected to ectopically express MCF_{Vv} fused to enhanced green fluorescent protein (EGFP) were rounded, but rounding was not accompanied by

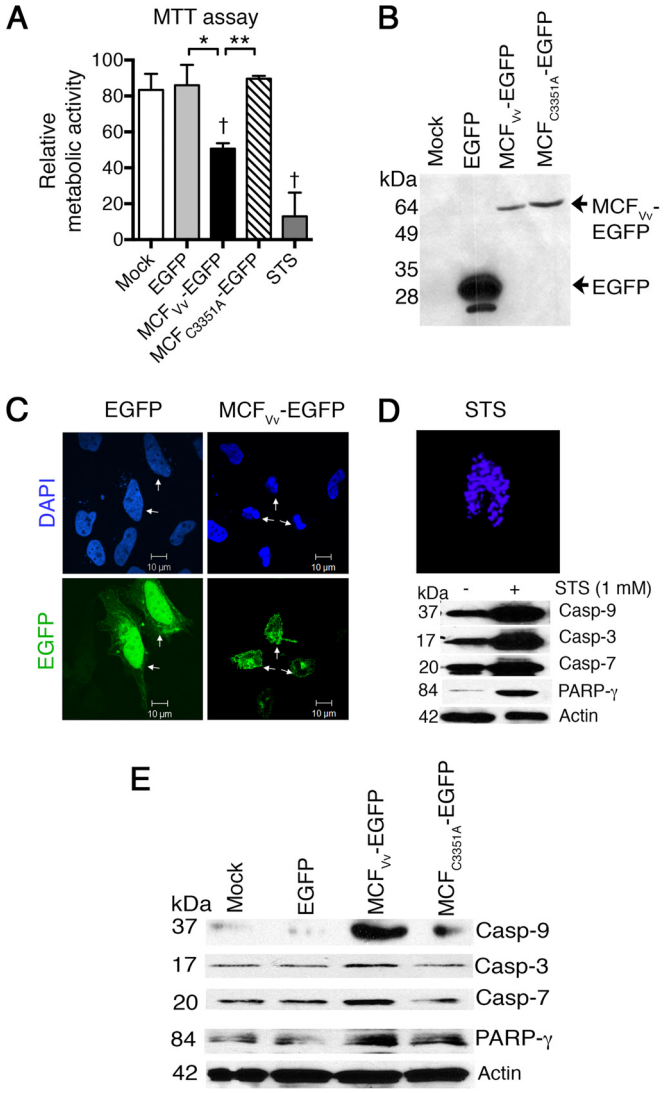

FIG 2 Ectopic expression of MCF_{Vv} inhibits host cell metabolic rate and induces caspase activation. (A) MTT assay on transfected HeLa cells. Data are presented as percent metabolic activity relative to untreated cells. "Mock" indicates cells treated with transfection reagent only. STS was used as a positive control. Results are means and SD for biological triplicates; daggers indicate statistical significance compared to mock-treated cells ($P < 0.05$), and asterisks show significant difference between the indicated samples (*, $P < 0.05$; **, $P < 0.01$). (B) Results of 12% SDS-PAGE showing expression of chimeric proteins by Western blotting using anti-EGFP antibody. (C) Nuclear staining with DAPI of HeLa cells transfected to express the indicated proteins. Arrowheads indicate transfected cells, as shown by detection of green fluorescence (EGFP). (D) DAPI staining of an STS-treated cell and detection of cleaved caspases as a positive control. (E) Representative Western blots of cell lysates from two independent experiments with HeLa cells transfected to express indicated EGFP fusion proteins. Actin is shown as a sample recovery control run in parallel gels along with other proteins.

LDH release, suggesting a cytopathic as opposed to a cytotoxic effect (26). To further establish how MCF_{Vv} affects host cells, the cellular metabolic activity in the transfected cells was measured by monitoring reduction of the tetrazolium dye MTT to detect the activity of NAD(P)/H-dependent oxidoreductase enzymes (33). In cells that were transfected to express MCF_{Vv} (Fig. 2A and B), ~50% of the cells lost their metabolic activity, consistent with a transfection frequency of 40 to 60% using our transfection method (Fig. 2B). In comparison, control cells expressing EGFP alone showed no difference in metabolic activity compared to the mock-transfected cells. The observed decrease in metabolic activity was due to active MCF_{Vv}, as cells transfected to express a variant of MCF_{Vv} rendered catalytically inactive by mutagenesis of the nucleophile cysteine to alanine (MCF_{C3351A}-EGFP) did not show a significant decrease in metabolic activity compared to the control. Treatment of cells for 1 h with 1 μM STS, a known inducer of apoptosis, completely abrogated cell metabolic activity (Fig. 2A). These data suggest that MCF_{Vv} not only induces cell rounding but is in fact cytotoxic, resulting in a dramatic loss of cell viability.

MCF_{Vv} induces cleavage of caspases and PARP-γ. Reduction of the tetrazolium ring of MTT to produce the dark blue formazan product can result from several types of cell death, including apoptosis (34). To determine if MCF_{Vv} stimulates apoptosis, cells transfected to express MCF_{Vv}-EGFP fusion protein were stained with DAPI to visualize the nuclear morphology. The MCF_{Vv} expression led to marked karyopyknosis (nuclear shrinkage) and karyorrhexis (nuclear fragmentation) (Fig. 2C), similar to STS-treated cells (Fig. 2D), a hallmark of cells undergoing apoptotic cell death. In comparison, EGFP-transfected cells showed healthy nuclei (Fig. 2C). These cells also showed normal localization of EGFP to the nuclei (35), while green fluorescence in cells expressing MCF_{Vv}-EGFP was localized to the cytosol, as previously described (26).

Lysates from the cells ectopically expressing MCF_{Vv}-EGFP were examined for the processing of procaspases as a marker of induction of apoptosis. In cells expressing MCF_{Vv}-EGFP, there was increased cleavage of the initiator caspase 9, as well as the downstream executioner caspase 3 and caspase 7 (Fig. 2E). There was also an increase of cleaved, inactive poly-(ADP-ribose) polymerase (PARP-γ), a nuclear protein normally involved in DNA repair. However, ectopic expression of catalytically inactive MCF_{C3351A}-EGFP showed minimal levels of processed caspases or PARP-γ, similar to results obtained with either mock- or *egfp*-transfected cells (Fig. 2E). As a control in a parallel experiment, treatment with STS was found to induce cleavage of caspases in these cells, as expected (Fig. 2D). This indicated that the MCF_{Vv}-induced cytotoxicity is coupled to activation of proapoptotic markers, suggesting that the MCF_{Vv} effector domain induces apoptosis.

Loss of cell proliferation and motility in cells intoxicated with LF_N-MCF_{Vv}. As the reduction of viability after ectopic expression could be exacerbated by MCF_{Vv} overexpression and subject to sample variation due to differences in transient-transfection frequencies, the effect of MCF_{Vv} on metabolic activity was further monitored using an alternative system which does not depend on transient gene expression and in which all cells in the pool are equally susceptible to treatment, facilitating a quantitative study. It was previously shown that MCF_{Vv} fused to the N terminus of anthrax toxin lethal factor (LF_N-MCF_{Vv}) can be introduced into cells by anthrax toxin PA, resulting in cell rounding. Addition of 72 pmol of LF_N-MCF_{Vv} at a 3:7 ratio with PA was not accompanied by cell lysis, as measured by LDH release (26). The MTT assay described above was extrapolated to the intoxication assay at this same dosage, but no significant differences were revealed dependent upon MCF_{Vv} (data not shown). To evaluate if cells treated with MCF_{Vv} can recover upon removal of toxin and proliferate, a clonogenic colony formation assay was performed

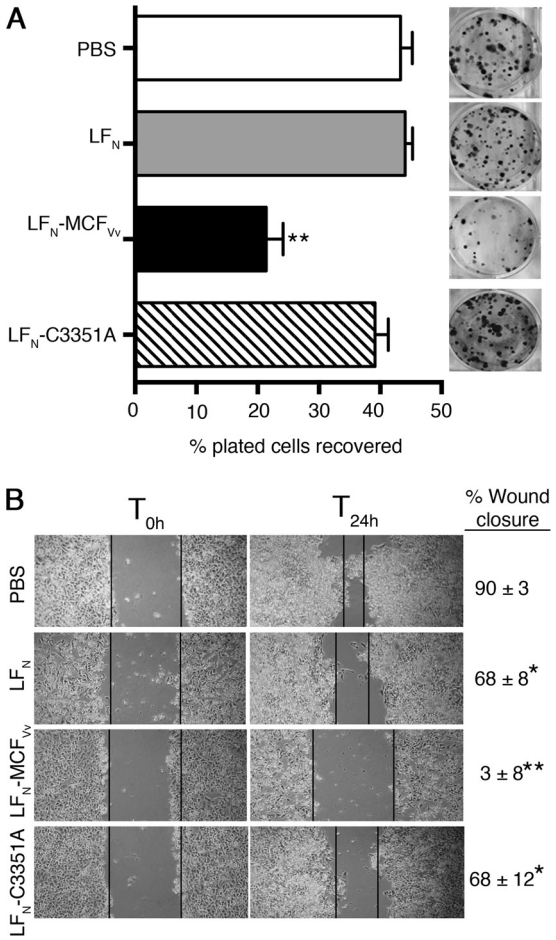

FIG 3 Direct delivery of MCF_{Vv} inhibits host cell proliferation and cell migration. (A) Clonogenic colony formation assay showing percentage of colonies recovered after intoxication with the indicated fusion proteins (72 nM) with PA (168 nM). The cells were seeded at densities of 200 and 400; the recovered colonies were counted, and percent survival was plotted. Quantitative data are reported as percentage of plated cells recovered (means and SD for four biological replicates, each plated twice). **, $P < 0.0001$ by ANOVA compared to all other samples. The inset shows one representative crystal violet-stained plate for each sample. (B) *In vitro* wound scratch assay showing photographs of migration patterns and rates of wound closure of HeLa cells within 24 h after intoxication (T_{24h}) with the indicated proteins. T_{0h} indicates the time of wound generation. Values on the right are percentage of the wound healed by cell migration, presented as means ± SD of the percent wound closure. *, $P < 0.05$, and **, $P < 0.0001$, by ANOVA followed by multiple comparison to the PBS-treated control.

with cells intoxicated for 24 h with LF_N fusion proteins and PA. Upon removal of toxin, cells were replated, and cells forming colonies were quantified. Only 23% of the cells treated with LF_N-MCF_{Vv} in the presence of PA were able to form colonies upon replating. By comparison, 44% of cells treated with LF_N alone were able to regrow. The ~50% inhibition of proliferation was due to the active MCF_{Vv}, since 39% of cells treated with the catalytically inactive LF_N-MCF_{C3351A} formed colonies (Fig. 3A). These data suggest that, in cells intoxicated with LF_N-MCF_{Vv}, about 50% of cells are permanently damaged, whereas about 50% can still recover. This result is consistent with our previous observation that about 55% of cells treated with LF_N-MCF_{Vv} showed pronounced rounding (26).

A corollary method was also utilized to monitor lack of cell growth and migration as a measure of cytotoxicity without the need to replate, so the cells could remain exposed to toxin over a longer period. After a scratch wound is introduced into the monolayers, cells at the wound edge are expected to polarize and migrate into the wound space in proportion to their viability index (30). Almost complete wound closure was observed within 24 h in PBS-treated cells (Fig. 3B). Similarly, control cells treated with unfused LF_N in the presence of PA showed wound closure, indicating that neither LF_N nor PA affected cell growth and migration. In contrast, cells exposed to LF_N-MCF_{Vv} in the presence of PA did not migrate into the wound site, and the width of the wound remained unchanged after 24 h (Fig. 3B). In fact, the width of the wound actually increased after 48 h, because cells began to lift off the plastic, making the wound edges indistinct (data not shown).

Overall, these data indicate that delivery of LF_N-MCF_{Vv} into cells led to impaired cell growth and motility, particularly with prolonged toxin exposure. In the case of overexpression, MCF_{Vv}-EGFP further led to significant loss of metabolic activity, as detected in the MTT assay (Fig. 2A). Furthermore, all growth and metabolic inhibition was dependent upon catalytically active MCF_{Vv}, linking these effects to the MCF_{Vv} activity (Fig. 2A and 3).

Caspase activation in cells intoxicated with LF_N-MCF_{Vv}. To determine if caspase activation is mediated by MCF_{Vv} upon LF_N-MCF_{Vv} intoxication as it is by ectopic expression, cell lysates intoxicated with LF_N-MCF_{Vv} for 24 h were monitored for caspase and PARP-γ cleavage. Cells treated with LF_N-MCF_{Vv} showed increased activation of caspases 9, 3, and 7 and inactivation of PARP-γ with at least a 5-fold stimulation over cells intoxicated with LF_N alone or cells treated with the catalytically inactive protein LF_N-C3351A (Fig. 4A and B). Moreover, in this case, the level of the precursor procaspase 9 was also found to be upregulated upon MCF_{Vv} exposure (Fig. 4A), indicating an anticipated increased conversion of the precursor into active caspase 9, similar to the hypoxia-induced apoptosis in cerebral cortex of piglets (36). Further, the effect was inhibited by incubation of cells with the pancaspase inhibitor z-VAD-fmk (Fig. 4A). These results indicate that cells undergo MCF_{Vv}-dependent caspase activation, even when the effector domain is delivered exogenously and not ectopically overexpressed.

Activation of the initiator caspase 9 can occur via either the intrinsic or the extrinsic apoptosis pathways (37). Extrinsic activation of caspases 9 and 3 is mediated through caspase 8 cleavage, which is initiated upon ligation of death receptors at the host cell membrane (38). However, no activation of caspase 8 was evident in cells intoxicated with LF_N-MCF_{Vv}, unlike in cells treated with cycloheximide followed by TNF-α, a treatment known to induce caspase 8 (39) (Fig. 4C). This result is consistent with studies using whole *V. vulnificus* bacteria wherein activation of apoptosis due to *rtxA1* occurred via the intrinsic pathway, not the extrinsic pathway (16).

MCF_{Vv} induces disruption of mitochondrial membrane potential. The intrinsic apoptotic pathway is induced by mitochondrial damage coupled to upregulation of proapoptotic proteins like Bax, Bak, and Bad and release of cytochrome *c*. Thus, we examined the effect of LF_N-MCF_{Vv} intoxication on mitochondrial transmembrane potential (Ψ_m) using JC-1, a positively charged potentiometric green fluorescent dye that accumulates in active healthy mitochondria as fluorescent red J aggregates in a potential-dependent manner. Therefore, apoptotic cells, which exhibit

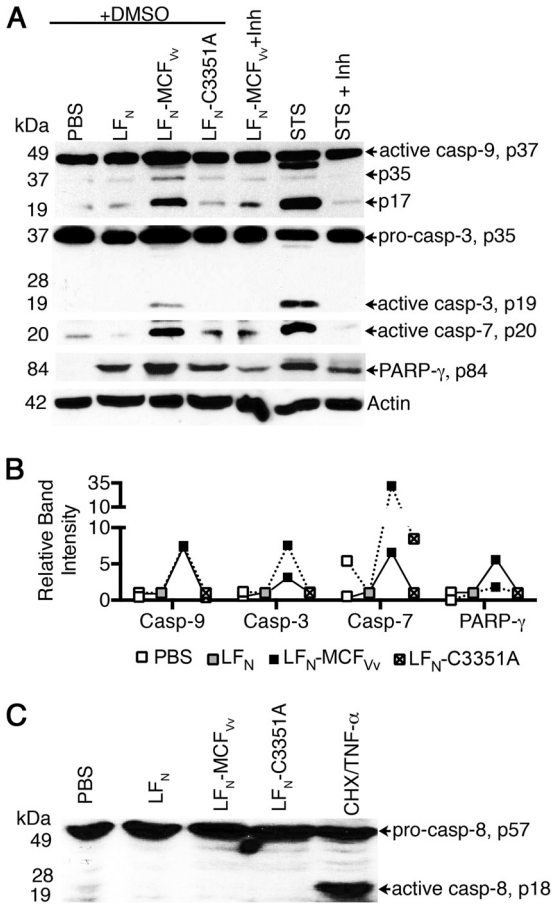

FIG 4 MCF$_{Vv}$ induces an intrinsic but not an extrinsic branch of apoptosis. (A) Representative Western blot showing processing of caspases and PARP-γ in HeLa cells intoxicated with the indicated LF$_N$ fusion proteins. Experiment were conducted in the presence of a pancaspase inhibitor (z-VAD-fmk; 100 μM, 4 h) or DMSO. STS (100 μM, 1 h) is shown as a positive control for detection of bands at appropriate size. (B) Relative densitometric quantification of the band intensities for each indicated protein relative to cells intoxicated with unfused LF$_N$ protein (gray box at 1.0). Data are from two independent experiments (linked by solid or dashed lines) conducted as for panel A except without DMSO or z-VAD-fmk. (C) Western blot showing activation of caspase 8 in HeLa cells intoxicated with the indicated fusion proteins. Cycloheximide (CHX)–TNF-α was used as a positive control for detection of appropriately sized bands. The arrows indicate procaspase 8 at 57 kDa and the cleaved fragment at 18 kDa.

primarily green fluorescence, can easily be differentiated from healthy cells, which show both red and green fluorescence. While cells with reduced Ψ_m showed an excess of green, as seen in the STS control (Fig. 5A and B), the confocal images of control HeLa cells treated only with PBS showed healthy cells with a strong stimulation of conversion of the green dye to red aggregates. In contrast, cells intoxicated with LF$_N$-MCF$_{Vv}$ after 24 h showed cell rounding and lacked red-orange J aggregates, and the dye appeared as a diffuse green cytosolic fluorescent signal, indicative of a JC-1 monomer. The ratio of red to green signal for the LF$_N$-MCF$_{Vv}$-treated cells showed a statistically significant excess of green, indicative of a lower Ψ_m and mitochondrial depolarization. The cells treated with either unfused LF$_N$ or LF$_N$-MCF$_{Vv}$ with a cysteine point mutation, however, showed robust aggregation of J aggregates in the mitochondria and excess red fluorescence similar to that observed for PBS controls (Fig. 5A and B).

Cytochrome *c* is generally sequestered in the intermembrane space of mitochondria, but it leaks into the cytosol when the mitochondrial permeability transition pore is damaged in response to Ψ_m collapse. Indeed, intoxication of cells with catalytically active LF$_N$-MCF$_{Vv}$ in the presence of PA led to 2- to 3-fold-increased release of cytochrome *c* in to cytosol compared to cells treated with LF$_N$ in the presence of PA with a correlated loss of 40 to 90% of cytochrome *c* from mitochondria (Fig. 5C). In addition, the lysates of LF$_N$-MCF$_{Vv}$-intoxicated cells, but not those intoxicated with the catalytically inactive mutant, showed induction of proapoptotic markers like Bax and Bak. Bad was also affected but to a lesser extent, and this effect was not consistently reproducible (Fig. 5D). The data reveal that MCF$_{Vv}$ is associated with induction of the intrinsic apoptotic cascade following mitochondrial damage.

Production of *V. vulnificus* strains that secrete a MARTX$_{Vv}$ toxin that delivers only MCF$_{Vv}$. These studies link MCF$_{Vv}$ to induction of mitochondrial damage and the intrinsic pathway for apoptosis. However, it is possible that this does not account for *rtxA1*-associated induction of apoptosis during coculture of bacteria with epithelial cells, which has previously been suggested as an indirect effect of altered cell signaling upon MARTX$_{Vv}$ pore formation or due to activities of other uncharacterized effector domains (16, 17). To directly link MCF$_{Vv}$-induced caspase activation to *V. vulnificus rtxA1*-mediated induction of apoptosis, a modified MARTX$_{Vv}$ toxin system that allows delivery of either no effectors or only one effector was employed (18, 20).

It was recently shown through modification of the *rtxA1* gene on the *V. vulnificus* chromosome that the repeats flanking the effector domains generate a pore in the eukaryotic cell plasma membrane through which the surrogate effector Bla can be delivered into the host cytosol in the absence of all other effector domains (*rtxA1*::*bla*) (18). The secretion of the translated toxin RtxA1::Bla from *V. vulnificus* into the medium can be monitored using ampicillin resistance of bacteria grown on LB, and translocation of the effector domain into eukaryotic cells can be quantified by loss of fluorescence resonance energy transfer (FRET) upon cleavage of the fluorogenic reagent CCF2-AM loaded into eukaryotic cells (18).

For this work, we modified the *rtxA1*::*bla* gene in *V. vulnificus* strain BS1407 (Fig. 6A) to introduce an in-frame fusion of *mcf*$_{Vv}$ within *rtxA1*::*bla* such that the resulting translated MARTX$_{Vv}$ toxin, RtxA1::MCF$_{Vv}$-Bla, gains either the effector domain MCF$_{Vv}$ (SNG1) or its catalytic mutant, MCF$_{C3351A}$ (SNG2) (Fig. 6A). The predicted natural processing sites of MCF$_{Vv}$ were retained in the construct such that the effector domain should be processed from the MARTX$_{Vv}$ holotoxin after translocation into the epithelial cells.

None of the strains with modified *rtxA1* genes showed a significant difference in growth in liquid broth compared to the isogenic *V. vulnificus* Δ*vvhA* parent strain BS1405, which produces a full-length RtxA1 toxin, the isogenic *rtxA1* null strain BS1406, or the *rtxA1*::*bla* strain BS1407 (Fig. 6A and B). Further, strains SNG1and SNG2, which secrete RtxA1::MCF$_{Vv}$-Bla or RtxA1::MCF$_{C3331A}$-Bla, respectively, gained ampicillin resistance comparable to that of the RtxA1::Bla strain BS1407 (Fig. 6C), indicating that the toxins are produced and secreted into the medium.

These strains were also translocation competent, as determined by transfer of Bla activity to HeLa cells. The *V. vulnificus* strain BS1407, secreting RtxA1::Bla, showed efficient transloca-

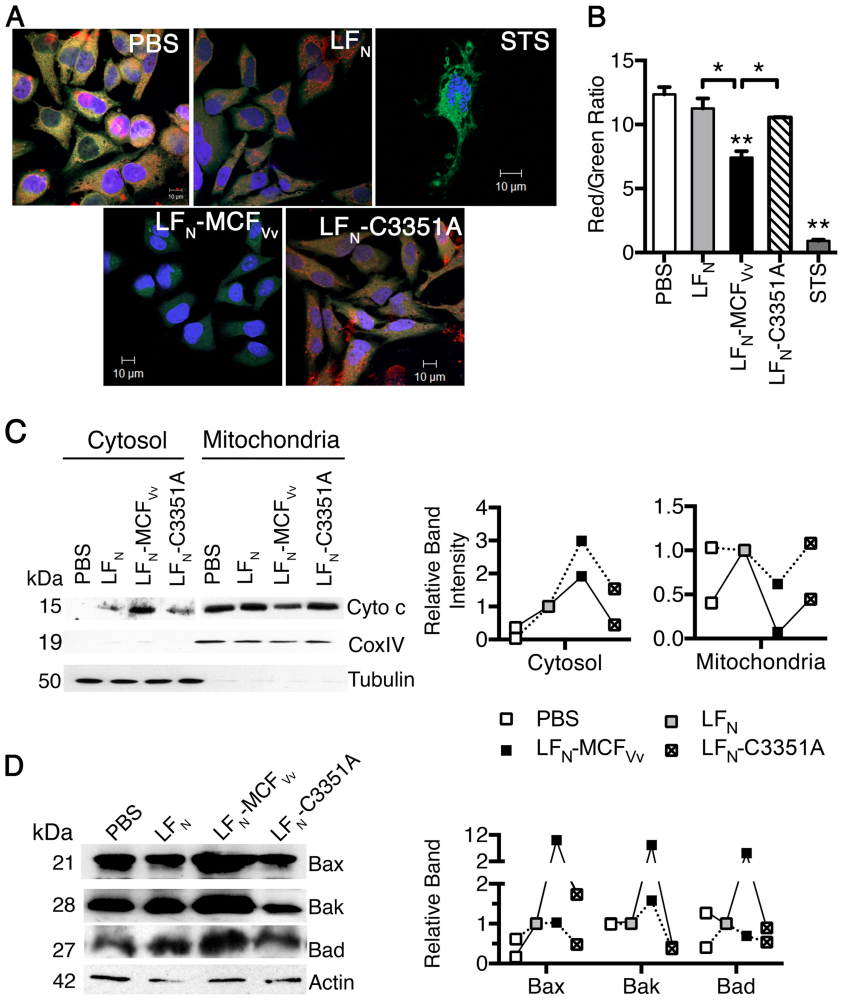

FIG 5 MCF$_{Vv}$ induces mitochondrial damage. (A) JC-1-stained live cells showing red-orange fluorescent aggregates in normal-appearing cells and diffused green fluorescence dispersed throughout the cytoplasm, with minimal red orange fluorescent aggregates in damaged cells. (B) Quantitation of fluorescence intensities from biological triplicate samples similar to those used for panel A was done by measuring the ratio of red (hyperpolarized) to green (depolarized) fluorescence. **, $P < 0.01$ compared to PBS control; *, $P < 0.05$ for the indicated comparisons. (C) Cell lysates were fractionated into cytosolic or mitochondria. Anti-cytochrome *c* antibody was used to probe the level of protein with CoxIV and tubulin proteins used as fractionation markers for mitochondria and cytosol, respectively. (D) Representative Western blots of cell lysates probed for expression levels of the indicated proteins, with actin used as a sample recovery control. On the right is a densitometric quantification of the band intensity for the indicated proteins from two independent experiments (linked by solid or dashed lines) relative to cells intoxicated with unfused LF$_N$ protein (gray boxes at 1.0).

tion of Bla from the toxin into HeLa cells with 68% of CCF2 loaded HeLa cells emitting blue fluorescence, indicative of Bla cleavage of CCF2 to disrupt FRET. The strains secreting either the catalytically active (SNG1) or inactive (SNG2) RtxA1::MCF$_{Vv}$-Bla toxins actually showed no significant difference, and at 85% and 88% blue cells, they actually transfer Bla to cells with slightly higher efficiency than BS1407 (Fig. 6D). This result is consistent with studies of *V. cholerae* RtxA::Bla translocation where it was found that introduction of any effector domain in front of Bla increased Bla translocation efficiency (20).

In conjunction with translocation, within the short time frame of this assay, HeLa cells did not lyse. However, with longer incubation, significant lysis of the HeLa cells by all of the *rtxA1*-modified strains was observed (Fig. 6E). At 120 and 150 min coincubation, the strains producing a RtxA1::MCF$_{Vv}$-Bla toxin induced a slightly enhanced cell lysis compared to the RtxA1::Bla-secreting strain BS1407, although the efficiency was still less than for the wild-type strain (Fig. 6E). As expected, since MCF$_{Vv}$ is suggested to induce not necrosis but apoptosis, there was no difference in cell lysis by catalytically active (SNG1) or inactive (SNG2) RtxA1::MCF$_{Vv}$-Bla toxins. Indeed, these data are consistent with previous observations that the N- and C-terminal repeat regions of the MARTX$_{Vv}$ toxin are both essential and sufficient for necrosis but that lysis is more efficient when all effector domains are present (18).

MCF$_{Vv}$ is the effector domain of MARTX$_{Vv}$ that induces mitochondrial damage. Having established that strains SNG1 and SNG2 can produce a translocation-competent MARTX$_{Vv}$ toxin carrying only a single effector domain, we tested if the gain of MCF$_{Vv}$, but not catalytically inactive MCF$_{Vv}$, in the MARTX$_{Vv}$ toxin correlated with induction of apoptosis. Strain SNG1 induced a loss of Ψ_m, as shown by a significant reduction in the conversion of the green JC1 dye to red J aggregates compared to that seen with SNG2 and with the controls RtxA1::Bla-secreting

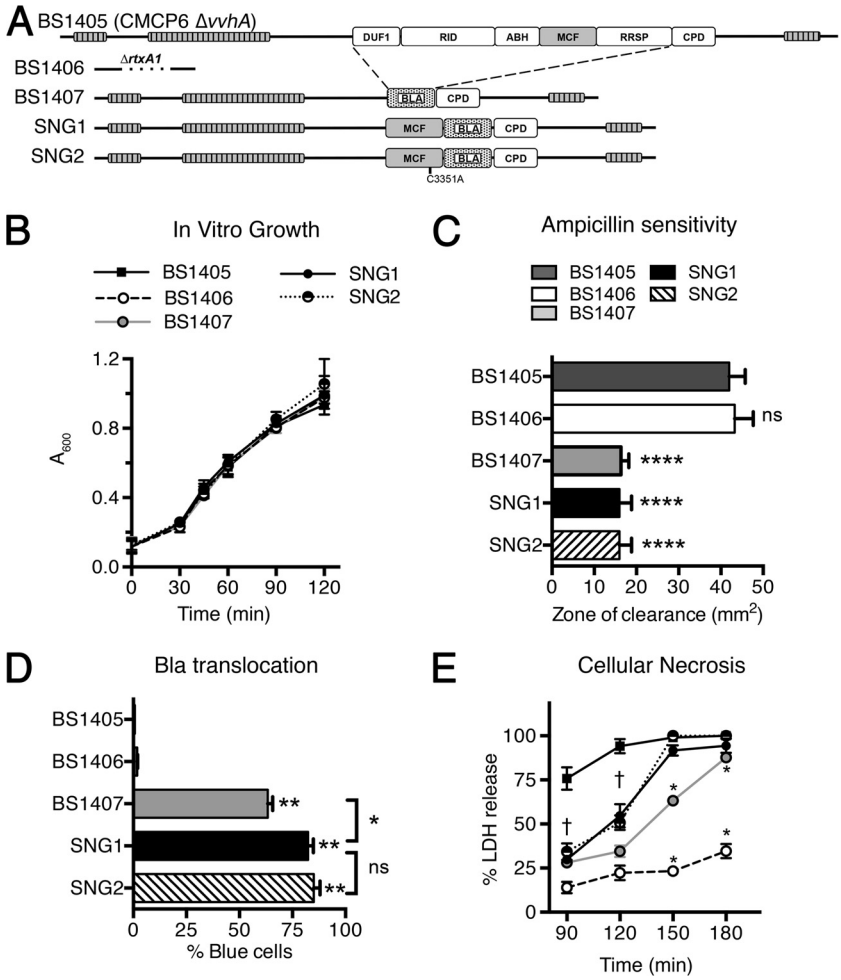

FIG 6 Modification of the $MARTX_{Vv}$ in *V. vulnificus* to deliver only the MCF_{Vv} effector domain. (A) Schematic representation of effector domains from the $MARTX_{Vv}$ toxin of *V. vulnificus* BS1405, a modified variant of CMCP6 with *vvhA* deleted. Effector domains are abbreviated as in Fig. 1. The replacement of all the effectors with Bla (BS1407), MCF_{Vv}-Bla (SNG1), or MCF_{C3351A}-Bla (SNG2) retains the repeat-containing regions, the C-terminal secretion signal sequence, and the CPD with its natural processing sites, including processing sites between MCF_{Vv} and Bla. (B) Absorbance of the indicated strains during growth in LB medium. (C) Resistance of Bla-producing strains to ampicillin in a disc assay. ****, $P < 0.0001$ compared to negative controls BS1405 and BS1406. (D) Translocation of the modified $MARTX_{Vv}$ toxins in the HeLa cell cytosol, as measured by gain of blue fluorescence, indicating intracellular cleavage of CCF2. The strains were cocultured with HeLa cells at an MOI of 10 for 60 min. **, $P < 0.005$ compared to negative controls BS1405 and BS1406. *, $P < 0.05$; ns, not significant. (E) Percentage LDH release from the cocultured HeLa cells with the indicated bacterial strains (MOI = 10) for the indicated times. For all assays, data are means and SD ($n = 3$). Daggers indicate that all values below are significantly different ($P < 0.05$) from the value for the BS1405 positive control. Asterisks indicate that only the indicated value is significantly different.

strain BS1407 and *rtxA1*-null strain BS1406 (Fig. 7A and B). Treatment of cells with SNG1 but not SNG2 also induced release of cytochrome *c* from mitochondria, with a parallel loss of cytochrome *c* from mitochondria (Fig. 7D), and increased expression of Bax and Bak, also with a slight increase in Bad (Fig. 7E). The mitochondrial damage stimulated caspase activation such that that SNG1 induces processing of caspases 9, 7, and 3 and PARP-γ at levels at least 2-fold greater than those induced by SNG2 (Fig. 7E).

Strain BS1407, which produces a toxin that translocates only Bla, did not induce mitochondrion-mediated apoptosis. Thus, the repeat regions of the $MARTX_{Vv}$ that are sufficient for cellular necrosis are not sufficient for induction of mitochondrial damage. Further, the toxin produced by SNG2 that differs from the active RtxA1::MCF_{Vv}-Bla by only a single mutation in the MCF_{Vv} catalytic cysteine residue did not show activation of these markers of intrinsic apoptosis (Fig. 7).

Although these data cannot exclude the contribution of any of the other four effector domains of the $MARTX_{Vv}$ holotoxin in inducing apoptosis, it is noteworthy that parent strain BS1405, which produces a full-length $MARTX_{Vv}$ toxin, induced loss of Ψ_m at levels similar to those seen with SNG1 (Fig. 7B and C), indicating a predominant contribution of MCF_{Vv} to induction of programmed cell death by the $MARTX_{Vv}$ toxin.

Cell rounding occurs independent of caspase activation. A number of bacterial toxins that directly induce cytopathic effects stimulate apoptosis as a downstream response to prolonged exposure to toxin (40). To determine if activation of the caspase cascade is direct or indirect, cells treated with LF_N-MCF_{Vv} in the presence of PA were visualized by phase-contrast microscopy.

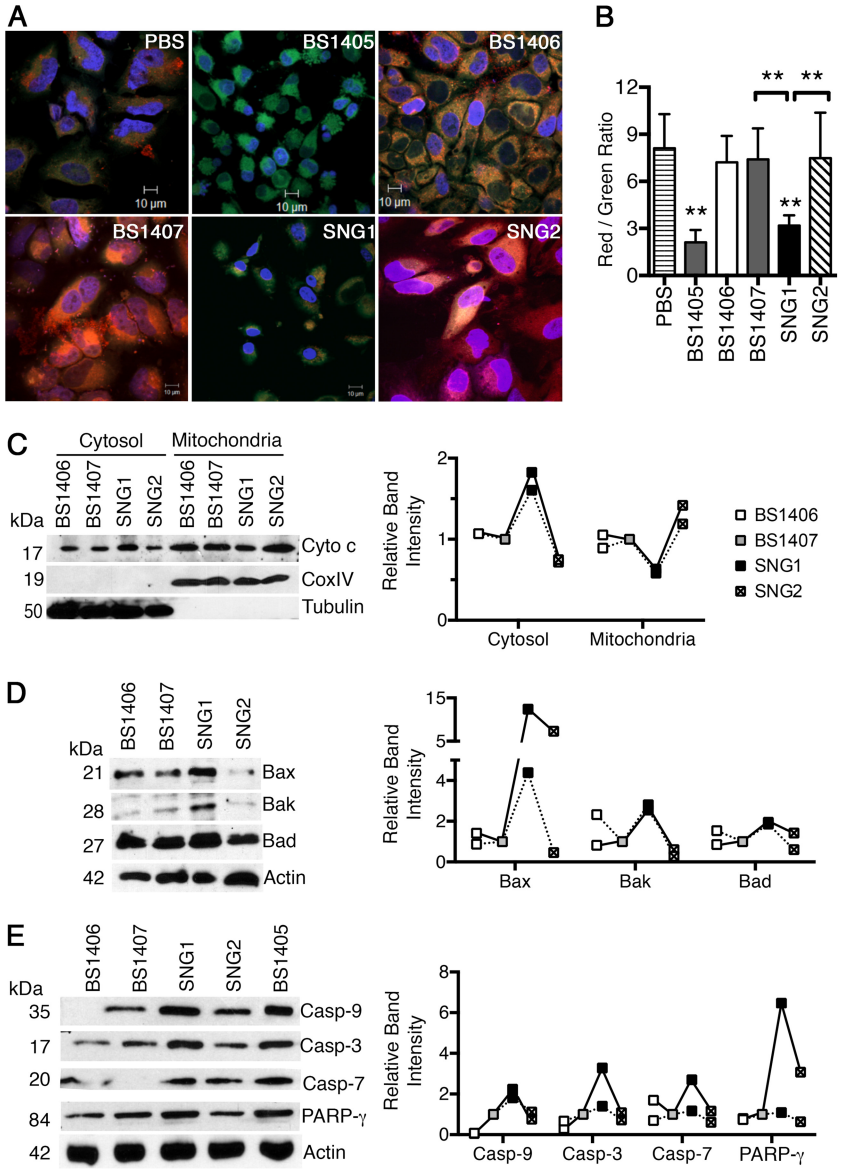

FIG 7 MCF_{Vv} is responsible for *V. vulnificus* mitochondrion-mediated induction of apoptosis. (A and B) HeLa cells cocultured with the indicated bacterial strains at an MOI of 10 for 60 min followed by a 30-min treatment with gentamicin to kill bacteria (90 min total) were stained with JC1 and quantified as described for Fig. 5. **, $P < 0.01$ compared to PBS control or indicated samples. (C) Western blot detection of cytochrome *c* in fractionated cell lysates (cytosol/mitochondria), prepared from cells cocultured with the indicated strains at an MOI of 10 for 90 min. CoxIV and tubulin proteins were used as fractionation markers for mitochondria and cytosol, respectively. (D and E) Western blot detection of indicated proteins from the HeLa cell lysates obtained after bacterial challenge with the indicated strains at an MOI of 10 for 90 min. Actin was used a sample recovery control. (C to E) Graphs show densitometric quantification of the band intensity for the indicated proteins. Data are representative of two independent experiments (linked by solid or dashed lines) and show intensity relative to that in cells treated with *rtxA1*::*bla* strain BS1407 (gray boxes at 1.0).

Treated cells were rounded as previously observed with about 50% proficiency dependent upon the LF_N-MCF_{Vv} catalytic cysteine (26). However, cells treated with the pancaspase inhibitor z-VAD-fmk prior to MCF_{Vv} exposure were also rounded (Fig. 8), although these cells showed no caspase activation (Fig. 4). Thus, the mechanism by which MCF_{Vv} induces the intrinsic pathway is likely a downstream indirect effect of the toxin's cytopathic activity, rather than MCF_{Vv} directly affecting mitochondrial membrane integrity. Thus, MCF_{Vv} is both a cytopathic and a cytotoxic effector domain that manipulates cell organization, resulting in the induction of cellular apoptosis.

DISCUSSION

Deletion of the *rtxA1* gene that encodes the $MARTX_{Vv}$ toxin from the pathogen *V. vulnificus* shows a significant 100- to 1,000-fold reduction in virulence, with the toxin being required for both colonization of the infection site and systemic spread (3–7). During coculture of bacteria with intestinal epithelial cells, the $MARTX_{Vv}$ toxin was shown to be the key factor for induction of apoptosis in an original study by Lee et al. (16). That study suggested a linkage of the effector domains to induction of apoptosis, although others suggested that the repeat regions are sufficient for

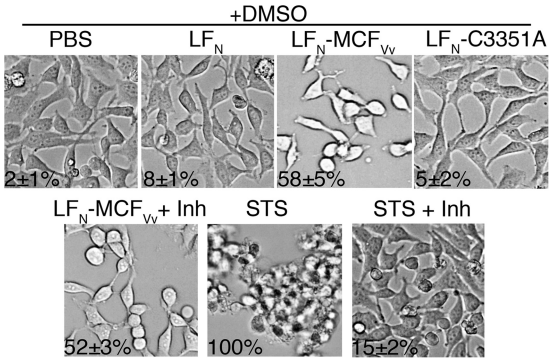

FIG 8 Cell rounding is not inhibited by the pancaspase inhibitor z-VAD-fmk (Inh). Bright-field images showing morphology of HeLa cells intoxicated with the indicated proteins in the presence of the pancaspase inhibitor z-VAD-fmk (100 μM, 4 h) or DMSO alone. Percent cell rounding was quantitated and is presented as mean ± SD ($n = 100$). This experiment was repeated simultaneously with the experiment whose results are shown in Fig. 3, so controls for caspase activation did not need to be presented twice.

programmed cell death, with effector domains being dispensable (17). However, there were indeed no previous studies that mapped the precise portion of MARTX$_{Vv}$ responsible for *V. vulnificus* induction of apoptosis. The present study was therefore carried out to specifically delineate the contribution of MARTX$_{Vv}$ in general, and effector domain(s) in particular, in eliciting programmed cell death.

In our recent study, we demonstrated MCF$_{Vv}$ to be a cytopathic effector domain that induces host cell rounding (26); however, the cell biological processes orchestrated by this putative cysteine protease remained unexplored. The importance of MCF$_{Vv}$ as an effector of *V. vulnificus* and its probable contribution to virulence are underscored by its ubiquitous presence in many clinical biotype 1 strains and also the occurrence of a duplication event in some biotype 1 strains as well as in biotype 2 strains that infect eels (Fig. 1) (21, 22). Notably, both biotype 1 and biotype 2 strains have been identified as inducing apoptosis (41). In the current study, MCF$_{Vv}$ ectopic expression (Fig. 2) or delivery (Fig. 4) to epithelial cells was found to reduce host cell proliferation and induced marked morphological and biochemical changes within the host, including cell rounding (Fig. 5 and 7). MCF$_{Vv}$ transfection or intoxication was also found to induce the intrinsic pathway of programmed cell death, as shown by disruption in mitochondrial transmembrane potential, activation and release of proapoptotic markers from the mitochondria, caspase activation, and nuclear condensation (Fig. 3 to 5). Overall, these results indicate that MCF$_{Vv}$ successfully alters host cell biology, resulting in both cytopathic and cytotoxic effects.

A key approach that distinguishes this work from previous studies linking rVVC (12–14) and VvpM (15) to apoptosis is that we were then able to link the induction of the intrinsic pathway of apoptosis by MCF$_{Vv}$ directly to the apoptotic phenotype that was observed when *V. vulnificus* was added to epithelial cells as opposed to purified proteins (16). This was possible because our laboratory has developed novel systems in both *V. cholerae* and *V. vulnificus* that facilitate segregation of the functional contribution of independent effector domains from the contributions of the MARTX toxin repeat-containing regions, the autoprocessing CPD, and other effector domains (18, 20). The use of Bla as a marker of translocation has further facilitated ongoing study of these toxins while circumventing the as-yet-unsolved technical barrier to studying effector domain translocation due to the inability of our or any other laboratory to purify the toxins or track effector domain processing *in vivo*, which thus far have been characterized exclusively *in vitro* (42).

In *V. vulnificus*, development of this system using the surrogate heterologous effector Bla revealed that both the N- and C-terminal repeat regions are essential for translocation of effector domains across the host cell plasma membrane (18). In the present study, we expanded the utility of this system to introduce a single MARTX$_{Vv}$ effector, MCF$_{Vv}$, while using the cotranslocated Bla as a reporter to monitor successful toxin secretion into the medium and translocation. Interestingly, in the course of developing the system for this project, we found that inclusion of MCF$_{Vv}$ in front of Bla in the RtxA1::MCF$_{Vv}$-Bla toxin resulted in both improved translocation and enhanced rates of MARTX$_{Vv}$-dependent cell lysis in comparison to the effectorless toxin strain. This effect was independent of the catalytic activity of MCF$_{Vv}$, indicating that the translocon generated by the MARTX$_{Vv}$ repeat regions functions more efficiently in the presence of an effector domain that generates a holotoxin structurally closer to the natural MARTX$_{Vv}$. A similar effect was also observed for *V. cholerae* MARTX$_{Vc}$, where the effect was far more pronounced (20). This difference may indicate that the highly stable *V. cholerae* MARTX (20) is evolutionarily more finely tuned to translocate its specific repertoire of three effector domains, while the *V. vulnificus* MARTX may show greater flexibility in acceptable effector domain cargo, consistent with the high rate of ongoing genetic exchange of effector domains occurring naturally in the environment (21, 22).

As a corollary conclusion to our finding that catalytically active MCF$_{Vv}$ is essential for MARTX$_{Vv}$-dependent induction of apoptosis, we also found that the repeat regions are not sufficient for this activity. In fact, we found that under the conditions of this study, there was a lack of plasma membrane rupture or leakage of cellular contents, as assessed by LDH release at a time point when caspase activation was evident. This is in contrast to a recent report by Kim et al. that showed that cells cocultured with *V. vulnificus* induced necrotic cell death in a caspase-independent manner coupled with mitochondrial dysfunction (17). In the present study, we observed reduction of Ψ_m and cleavage of caspases in a MARTX$_{Vv}$-dependent fashion, contrary to the observations by Kim et al. (17). This apparent discrepancy could be due to their use of strain M06-24/O, which has a slightly different repertoire of effector domains (Fig. 1), or our use of a strain background with the gene *vvhA* deleted to avoid inappropriate assignment of phenotypes to VVC. More likely, however, is that in the study by Kim et al. (17), bacterial challenge was performed at a high MOI of 100, rather the lower MOI of 10 used in this study and also by Lee et al. (16). Under these low-toxin-exposure conditions, we observed no cell lysis until later time points, but we did observe evidence of mitochondrial damage and activation of apoptotic markers in an MCF$_{Vv}$-dependent fashion, closely matching the phenotypes reported by Lee et al. (16) as being due to the MARTX$_{Vv}$ holotoxin. These effects at low MOI likely more closely reflect the *in vivo* situation, especially during early infection, with necrosis occurring only late in infection when the bacterial load is very high.

At present, it remains to be determined whether MCF$_{Vv}$ directly interacts with mitochondrial components and perturbs its physiology or acts indirectly. Several toxins are known that spe-

cifically target mitochondria by manipulating mitochondrial dynamics, including VacA from *Helicobacter pylori* (43) and the T3SS effector VopE from *V. cholerae* (44). However, Western blotting of cytosolic and membrane fractionation of HeLa cells transfected to express MCF_{Vv} did not reveal significant partitioning of MCF_{Vv} in the membrane (data not shown). In addition, localization of catalytically inactive MCF_{Vv} in HeLa cells suggested colocalization with a subcellular organelle, and the localization pattern did not match that expected of mitochondrial colocalization (26).

Further suggesting that MCF_{Vv} does not directly target mitochondrial dynamics or membrane is that the cell rounding phenotype induced by delivery of LF_N-MCF_{Vv} to cells was not dependent on activation of caspases. This suggests that caspases were activated as an indirect consequence of MCF_{Vv}-induced cell rounding. This is known to occur for *Clostridium difficile* toxin B (TcdB), which UDP-glucosylates Rho GTPases, resulting in cytoskeletal disruption and altered transcription of antiapoptotic genes with a downstream consequence of induction of apoptosis (40, 45). Similarly, constitutive activation of Rac and Cdc42 by the *E. coli* cytotoxic necrotizing factor 1 (CNF1) also results in cell death upon prolonged toxin exposure (46). While these examples point to possible mechanisms of action for MCF_{Vv}, we did not observe any change in the activation state of RhoA, Rac1, or Cdc42 at either 4 h or 24 h after exposure of cells to LF_N-MCF_{Vv} in the presence of PA (data not shown). Thus, it is possible that MCF_{Vv} has a novel target for processing or covalent modification resulting in cell rounding and subsequent activation of apoptosis. Studies are in progress to identify the host component that is directly targeted by MCF_{Vv} in order to activate this branch of pathway within the host.

Finally, although MCF_{Vv} was mapped as the predominant effector within $MARTX_{Vv}$ toxin responsible for inducing an apoptotic phenotype, we speculate that while MCF_{Vv} is sufficient to induce apoptosis, other effector domains may have overlapping functions and also induce apoptosis either directly or indirectly. The neighboring Ras/Rap1 specific protease (RRSP) effector domain in the $MARTX_{Vv}$ toxin of CMCP6 used here has recently been shown to induce cell rounding (47) but also to cleave RAS, a small GTPase that controls ERK1/2 (48). In the absence of active RAS, cells are induced to undergo apoptosis via AKT (49, 50). DUF1 has also been linked recently to effects on mitogen-activated protein kinase signaling through its binding to prohibitin 1 (51). Similarly, inactivation of RhoA by the second effector domain within $MARTX_{Vv}$ that is similar to RID_{Vc} (52) could conceivably be coupled with induction of apoptosis, as occurs also for TcdB-mediated RhoA inactivation. We propose that future study of individual effector or effector domain combinations using this delivery mechanism will enhance our understanding of the exclusive, synergistic, or antagonistic contribution of these effector domains sandwiched within the $MARTX_{Vv}$ holotoxin, which is known to induce a plethora of cytopathic and cytotoxic effects.

ACKNOWLEDGMENTS

We thank Shivani Agarwal for providing the protective antigen (PA), Jennifer Wong for technical assistance, the Northwestern Genomics Core for DNA sequencing services, the Immunobiology Center for flow cytometry instrumentation, and the Center for Advanced Microscopy for microscopy instrumentation.

This work was supported by National Institutes of Health grants R01AI092825 and R01AI098369 (to K.J.F.S.) and by grants R01CA152601, R01CA152799, and R01CA168292 and a Northwestern University Avon Center of Excellence grant (to D.R.G.).

REFERENCES

1. **Jones MK, Oliver JD.** 2009. *Vibrio vulnificus*: disease and pathogenesis. Infect Immun **77:**1723–1733. http://dx.doi.org/10.1128/IAI.01046-08.
2. **Daniels NA.** 2011. *Vibrio vulnificus* oysters: pearls and perils. Clin Infect Dis **52:**788–792. http://dx.doi.org/10.1093/cid/ciq251.
3. **Kim YR, Lee SE, Kook H, Yeom JA, Na HS, Kim SY, Chung SS, Choy HE, Rhee JH.** 2008. *Vibrio vulnificus* RTX toxin kills host cells only after contact of the bacteria with host cells. Cell Microbiol **10:**848–862. http://dx.doi.org/10.1111/j.1462-5822.2007.01088.x.
4. **Lo HR, Lin JH, Chen YH, Chen CL, Shao CP, Lai YC, Hor LI.** 2011. RTX toxin enhances the survival of *Vibrio vulnificus* during infection by protecting the organism from phagocytosis. J Infect Dis **203:**1866–1874. http://dx.doi.org/10.1093/infdis/jir070.
5. **Lee JH, Kim MW, Kim BS, Kim SM, Lee BC, Kim TS, Choi SH.** 2007. Identification and characterization of the *Vibrio vulnificus rtxA* essential for cytotoxicity *in vitro* and virulence in mice. J Microbiol **45:**146–152.
6. **Liu M, Alice AF, Naka H, Crosa JH.** 2007. The HlyU protein is a positive regulator of *rtxA1*, a gene responsible for cytotoxicity and virulence in the human pathogen *Vibrio vulnificus*. Infect Immun **75:**3282–3289. http://dx.doi.org/10.1128/IAI.00045-07.
7. **Jeong HG, Satchell KJ.** 2012. Additive function of *Vibrio vulnificus* $MARTX_{Vv}$ and VvhA cytolysins promotes rapid growth and epithelial tissue necrosis during intestinal infection. PLoS Pathog **8:**e1002581. http://dx.doi.org/10.1371/journal.ppat.1002581.
8. **Wright AC, Morris JG, Jr.** 1991. The extracellular cytolysin of *Vibrio vulnificus*: inactivation and relationship to virulence in mice. Infect Immun **59:**192–197.
9. **Fan JJ, Shao CP, Ho YC, Yu CK, Hor LI.** 2001. Isolation and characterization of a *Vibrio vulnificus* mutant deficient in both extracellular metalloprotease and cytolysin. Infect Immun **69:**5943–5948. http://dx.doi.org/10.1128/IAI.69.9.5943-5948.2001.
10. **Kashimoto T, Ueno S, Hanajima M, Hayashi H, Akeda Y, Miyoshi S, Hongo T, Honda T, Susa N.** 2003. *Vibrio vulnificus* induces macrophage apoptosis in vitro and in vivo. Infect Immun **71:**533–535. http://dx.doi.org/10.1128/IAI.71.1.533-535.2003.
11. **Kuo SY, Chou MC, Lee SL, Wang Y, Chen CL, Lin PT, Lo HR.** 2015. *Vibrio vulnificus* RtxA1 modulated calcium flux contributes reduced internalization in phagocytes. Life Sci **132:**55–60. http://dx.doi.org/10.1016/j.lfs.2015.03.027.
12. **Zhao JF, Sun AH, Ruan P, Zhao XH, Lu MQ, Yan J.** 2009. Vibrio vulnificus cytolysin induces apoptosis in HUVEC, SGC-7901 and SMMC-7721 cells via caspase-9/3-dependent pathway. Microb Pathog **46:**194–200. http://dx.doi.org/10.1016/j.micpath.2008.12.005.
13. **Sun J, Zheng J, Wang G, Li Y, Shen H.** 2012. Apoptotic effect of *Vibrio vulnificus* cytolysin on A549 human lung adenocarcinoma cells. Mol Med Rep **5:**668–674. http://dx.doi.org/10.3892/mmr.2011.690.
14. **Lee SJ, Jung YH, Oh SY, Song EJ, Choi SH, Han HJ.** 2015. *Vibrio vulnificus* VvhA induces NF-kappaB-dependent mitochondrial cell death via lipid raft-mediated ROS production in intestinal epithelial cells. Cell Death Dis **6:**1655. http://dx.doi.org/10.1038/cddis.2015.19.
15. **Lee MA, Kim JA, Yang YJ, Shin MY, Park SJ, Lee KH.** 2014. VvpM, an extracellular metalloprotease of *Vibrio vulnificus*, induces apoptotic death of human cells. J Microbiol **52:**1036–1043. http://dx.doi.org/10.1007/s12275-014-4531-0.
16. **Lee BC, Choi SH, Kim TS.** 2008. *Vibrio vulnificus* RTX toxin plays an important role in the apoptotic death of human intestinal epithelial cells exposed to Vibrio vulnificus. Microbes Infect **10:**1504–1513. http://dx.doi.org/10.1016/j.micinf.2008.09.006.
17. **Kim YR, Lee SE, Kang IC, Nam KI, Choy HE, Rhee JH.** 2013. A bacterial RTX toxin causes programmed necrotic cell death through calcium-mediated mitochondrial dysfunction. J Infect Dis **207:**1406–1415. http://dx.doi.org/10.1093/infdis/jis746.
18. **Kim BS, Gavin HE, Satchell KJ.** 2015. Distinct roles of the repeat-containing regions and effector domains of the *Vibrio vulnificus* multifunctional-autoprocessing repeats-in-toxin (MARTX) toxin. mBio **6:**e00324-15. http://dx.doi.org/10.1128/mBio.00324-15.
19. **Satchell KJ.** 2011. Structure and function of MARTX toxins and other large repetitive RTX proteins. Annu Rev Microbiol **65:**71–90. http://dx.doi.org/10.1146/annurev-micro-090110-102943.

20. **Dolores JS, Agarwal S, Egerer M, Satchell KJ.** 2015. *Vibrio cholerae* MARTX toxin heterologous translocation of beta-lactamase and roles of individual effector domains on cytoskeleton dynamics. Mol Microbiol **95:**590–604. http://dx.doi.org/10.1111/mmi.12879.
21. **Kwak JS, Jeong HG, Satchell KJ.** 2011. *Vibrio vulnificus rtxA1* gene recombination generates toxin variants with altered potency during intestinal infection. Proc Natl Acad Sci U S A **108:**1645–1650. http://dx.doi.org/10.1073/pnas.1014339108.
22. **Roig FJ, Gonzalez-Candelas F, Amaro C.** 2011. Domain organization and evolution of multifunctional autoprocessing repeats-in-toxin (MARTX) toxin in *Vibrio vulnificus*. Appl Environ Microbiol **77:**657–668. http://dx.doi.org/10.1128/AEM.01806-10.
23. **Ziolo KJ, Jeong HG, Kwak JS, Yang S, Lavker RM, Satchell KJ.** 2014. *Vibrio vulnificus* biotype 3 multifunctional autoprocessing RTX toxin is an adenylate cyclase toxin essential for virulence in mice. Infect Immun **82:**2148–2157. http://dx.doi.org/10.1128/IAI.00017-14.
24. **Daborn PJ, Waterfield N, Silva CP, Au CP, Sharma S, Ffrench-Constant RH.** 2002. A single *Photorhabdus* gene, makes caterpillars floppy (mcf), allows *Escherichia coli* to persist within and kill insects. Proc Natl Acad Sci U S A **99:**10742–10747. http://dx.doi.org/10.1073/pnas.102068099.
25. **Pechy-Tarr M, Bruck DJ, Maurhofer M, Fischer E, Vogne C, Henkels MD, Donahue KM, Grunder J, Loper JE, Keel C.** 2008. Molecular analysis of a novel gene cluster encoding an insect toxin in plant-associated strains of Pseudomonas fluorescens. Environ Microbiol **10:**2368–2386. http://dx.doi.org/10.1111/j.1462-2920.2008.01662.x.
26. **Agarwal S, Agarwal S, Biancucci M, Satchell KJ.** 23 April 2015. Induced autoprocessing of the cytopathic Makes Caterpillars Floppy-like effector domain of the *Vibrio vulnificus* MARTX toxin. Cell Microbiol. http://dx.doi.org/10.1111/cmi.12451.
27. **Waterfield NR, Daborn PJ, Dowling AJ, Yang G, Hares M, ffrench-Constant RH.** 2003. The insecticidal toxin makes caterpillars floppy 2 (Mcf2) shows similarity to HrmA, an avirulence protein from a plant pathogen. FEMS Microbiol Lett **229:**265–270. http://dx.doi.org/10.1016/S0378-1097(03)00846-2.
28. **Vlisidou I, Dowling AJ, Evans IR, Waterfield N, ffrench-Constant RH, Wood W.** 2009. *Drosophila* embryos as model systems for monitoring bacterial infection in real time. PLoS Pathog **5:**e1000518. http://dx.doi.org/10.1371/journal.ppat.1000518.
29. **Mosmann T.** 1983. Rapid colorimetric assay for cellular growth and survival: application to proliferation and cytotoxicity assays. J Immunol Methods **65:**55–63. http://dx.doi.org/10.1016/0022-1759(83)90303-4.
30. **Cory G.** 2011. Scratch-wound assay. Methods Mol Biol **769:**25–30. http://dx.doi.org/10.1007/978-1-61779-207-6_2.
31. **Fullner KJ, Mekalanos JJ.** 1999. Genetic characterization of a new type IV-A pilus gene cluster found in both classical and El Tor biotypes of Vibrio cholerae. Infect Immun **67:**1393–1404.
32. **Waterhouse NJ, Steel R, Kluck R, Trapani JA.** 2004. Assaying cytochrome c translocation during apoptosis. Methods Mol Biol **284:**307–313.
33. **Slater TF, Sawyer B, Straeuli U.** 1963. Studies on succinate-tetrazolium reductase systems. Iii Points of coupling of four different tetrazolium salts Biochim Biophys Acta **77:**383–393.
34. **Shi Q, Hao L, Pei J, Yin W.** 2012. Promotion of apoptosis does not necessarily mean inhibition of remodeling. Hypertension **60:**e3. http://dx.doi.org/10.1161/HYPERTENSIONAHA.112.195784.
35. **Seibel NM, Eljouni J, Nalaskowski MM, Hampe W.** 2007. Nuclear localization of enhanced green fluorescent protein homomultimers. Anal Biochem **368:**95–99. http://dx.doi.org/10.1016/j.ab.2007.05.025.
36. **Delivoria-Papadopoulos M, Ashraf QM, Mishra OP.** 2008. Effect of hypoxia on the expression of procaspase-9 and procaspase-3 in neuronal nuclear, mitochondrial and cytosolic fractions of the cerebral cortex of newborn piglets. Neurosci Lett **438:**38–41. http://dx.doi.org/10.1016/j.neulet.2008.03.078.
37. **Parrish AB, Freel CD, Kornbluth S.** 2013. Cellular mechanisms controlling caspase activation and function. Cold Spring Harb Perspect Biol **5:**a008672. http://dx.doi.org/10.1101/cshperspect.a008672.
38. **Cullen SP, Martin SJ.** 2009. Caspase activation pathways: some recent progress. Cell Death Differ **16:**935–938. http://dx.doi.org/10.1038/cdd.2009.59.
39. **Wang L, Du F, Wang X.** 2008. TNF-alpha induces two distinct caspase-8 activation pathways. Cell **133:**693–703. http://dx.doi.org/10.1016/j.cell.2008.03.036.
40. **Fiorentini C, Falzano L, Travaglione S, Fabbri A.** 2003. Hijacking Rho GTPases by protein toxins and apoptosis: molecular strategies of pathogenic bacteria. Cell Death Differ **10:**147–152. http://dx.doi.org/10.1038/sj.cdd.4401151.
41. **Murciano C, Hor LI, Amaro C.** 2015. Host-pathogen interactions in *Vibrio vulnificus*: responses of monocytes and vascular endothelial cells to live bacteria. Future Microbiol **10:**471–487. http://dx.doi.org/10.2217/fmb.14.136.
42. **Pfeifer G, Schirmer J, Leemhuis J, Busch C, Meyer DK, Aktories K, Barth H.** 2003. Cellular uptake of Clostridium difficile toxin B. Translocation of the N-terminal catalytic domain into the cytosol of eukaryotic cells. J Biol Chem **278:**44535–44541.
43. **Jain P, Luo ZQ, Blanke SR.** 2011. *Helicobacter pylori* vacuolating cytotoxin A (VacA) engages the mitochondrial fission machinery to induce host cell death. Proc Natl Acad Sci U S A **108:**16032–16037. http://dx.doi.org/10.1073/pnas.1105175108.
44. **Suzuki M, Danilchanka O, Mekalanos JJ.** 2014. *Vibrio cholerae* T3SS effector VopE modulates mitochondrial dynamics and innate immune signaling by targeting Miro GTPases. Cell Host Microbe **16:**581–591. http://dx.doi.org/10.1016/j.chom.2014.09.015.
45. **Hippenstiel S, Schmeck B, N'Guessan PD, Seybold J, Krull M, Preissner K, Eichel-Streiber CV, Suttorp N.** 2002. Rho protein inactivation induced apoptosis of cultured human endothelial cells. Am J Physiol Lung Cell Mol Physiol **283:**L830–L838. http://dx.doi.org/10.1152/ajplung.00467.2001.
46. **Mills M, Meysick KC, O'Brien AD.** 2000. Cytotoxic necrotizing factor type 1 of uropathogenic Escherichia coli kills cultured human uroepithelial 5637 cells by an apoptotic mechanism. Infect Immun **68:**5869–5880. http://dx.doi.org/10.1128/IAI.68.10.5869-5880.2000.
47. **Antic I, Biancucci M, Satchell KJ.** 2014. Cytotoxicity of the *Vibrio vulnificus* MARTX toxin effector DUF5 is linked to the C2A subdomain. Proteins **82:**2643–2656. http://dx.doi.org/10.1002/prot.24628.
48. **Antic I, Biancucci M, Zhu Y, Gius D, Satchell KJ.** 2015. Site-specific processing of Ras and Rap1 Switch I by a MARTX toxin effector domain. Nat Commun **6:**7396. http://dx.doi.org/10.1038/ncomms8396.
49. **Gao N, Budhraja A, Cheng S, Liu EH, Huang C, Chen J, Yang Z, Chen D, Zhang Z, Shi X.** 2011. Interruption of the MEK/ERK signaling cascade promotes dihydroartemisinin-induced apoptosis in vitro and in vivo. Apoptosis **16:**511–523. http://dx.doi.org/10.1007/s10495-011-0580-6.
50. **Shan R, Price JO, Gaarde WA, Monia BP, Krantz SB, Zhao ZJ.** 1999. Distinct roles of JNKs/p38 MAP kinase and ERKs in apoptosis and survival of HCD-57 cells induced by withdrawal or addition of erythropoietin. Blood **94:**4067–4076.
51. **Kim BA, Lim JY, Rhee JH, Kim YR.** 1 July 2015. Characterization of prohibitin 1 as a host partner of *Vibrio vulnificus* RtxA1 toxin. J Infect Dis http://dx.doi.org/10.1093/infdis/jiv362.
52. **Ahrens S, Geissler B, Satchell KJ.** 2013. Identification of a His-Asp-Cys catalytic triad essential for function of the Rho inactivation domain (RID) of *Vibrio cholerae* MARTX toxin. J Biol Chem **288:**1397–1408. http://dx.doi.org/10.1074/jbc.M112.396309.